Available online at www.sciencedirect.com
ScienceDirect
Journal of the European Ceramic Society 27 (2007) 2495–2501
www.elsevier.com/locate/jeurceramsoc

Evolution of structure during the oxidation of zirconium diboride–silicon carbide in air up to 1500 °C

Alireza Rezaie [1], William G. Fahrenholtz *, Gregory E. Hilmas

Department of Materials Science and Engineering, 222 McNutt Hall, University of Missouri Rolla, Rolla, MO 65409, United States

Received 22 June 2006; received in revised form 25 September 2006; accepted 7 October 2006
Available online 29 November 2006

Abstract

The structures that developed as dense ZrB_2–SiC ceramics were heated to 1500 °C in air were characterized using scanning electron microscopy (SEM), energy dispersive spectroscopy (EDS) and X-ray diffraction. The oxidation behavior was also studied using thermal gravimetric analysis (TGA). Below 1200 °C, a protective B_2O_3-rich scale was observed on the surface. At 1200 °C and above, the B_2O_3 evaporated and the SiO_2-rich scale that formed was stable up to at least 1500 °C. Beneath the surface, layers that were rich in zirconium oxide, and from which the silicon carbide had been partially depleted, were observed. The observations were consistent with the oxidation sequence recorded by thermal gravimetric analysis.

Keywords: Borides; Composites; Oxidation

1. Introduction

Ceramic compounds such as ZrB_2, ZrC, TaC, HfB_2, HfC and HfN belong to a group of materials known as ultra high temperature ceramics (UHTCs). Interest in UHTCs has increased substantially in recent years due to growing interest in hypersonic vehicles and re-usable atmospheric re-entry vehicles.[1–11] For these vehicles, materials that are resistant to oxidation at 1500 °C and above are needed for a variety of components such as nose cones, wing leading edges and engine cowls.[4] Currently, UHTCs are among the candidates for these applications as well as other applications that require stability in extreme environments.[12–14]

As a family of compounds, UHTCs have high melting temperatures (>3000 °C) and they maintain their strength at elevated temperatures. With a theoretical density of 6.09 g/cm^3, ZrB_2 has the lowest density of the UHTCs,[15] which is a desired property for aerospace applications. In addition, ZrB_2 has a high thermal conductivity (65–135 W/m K) and has been reported to exhibit excellent thermal shock resistance.[15]

When ZrB_2–SiC is exposed to oxidizing environments at high temperatures, it oxidizes.[16,17] Several authors have reported that oxidation of ZrB_2–SiC at 1500 °C in air produces a structure that consists of four layers: (1) a continuous silica layer on the surface; (2) a Zr-rich oxidized layer embedded in amorphous silica; (3) a layer of SiC-depleted ZrB_2; (4) unaffected ZrB_2–SiC.[16,18,19] A thermodynamic model has been developed to understand the formation of this layered structure.[20] In the model, the steady-state response of ZrB_2–SiC to oxidation in air at 1500 °C was analyzed with the aid of ZrB_2 and SiC volatility diagrams. However, the development of the layered structure on the surface of ZrB_2–SiC as it is heated in air to 1500 °C and the transient structures that evolve during heating have not been investigated in detail.

The purpose of this paper is to describe the structures that develop when ZrB_2 containing 30 vol% SiC is heated in air. The compositions of the surface oxides that form during oxidation of ZrB_2–SiC are characterized for temperatures ranging from room temperature up to 1500 °C.

2. Experimental procedure

2.1. Processing

Commercially available ZrB_2 (Grade B, H.C. Starck, Newton, MA) with a reported purity of >99% (metals basis) and an averaged particle size of 2 μm was used. The SiC powder (Grade UF-10, H.C. Starck, Newton, MA) was predominantly

* Corresponding author. Tel.: +1 573 341 6343; fax: +1 573 341 6934.
E-mail address: billf@umr.edu (W.G. Fahrenholtz).
[1] Present address: Vesuvius, Beaver Falls, PA, United States.

0955-2219/$ – see front matter © 2006 Elsevier Ltd. All rights reserved.
doi:10.1016/j.jeurceramsoc.2006.10.012

α-SiC, and it had a reported purity of 98.5% and an average particle size of 0.7 μm. Batches containing 70 vol% ZrB_2 and 30 vol% SiC were prepared. Powders were attrition milled (Model 01-HD, Union Process, Akron, OH) for 2 h in hexane using ZrO_2 milling media (~3.5 mm diameter) to reduce particle size and promote intimate mixing. Solvent was removed by rotary evaporation (Model Rotavapor R-124, Buchi, Flawil, Germany) at a temperature of 70 °C, a vacuum of 200 mmHg (~27 kPa), and a rotation speed of 150 rpm. Rotary evaporation was utilized to minimize segregation due to differences in the sedimentation rates of the two powders, which have drastically different densities (6.1 g/cm^3 for ZrB_2 and 3.2 g/cm^3 for SiC).

Milled powders were hot-pressed (Model HP-3060, Thermal Technology, Santa Rosa, CA) at 1950 °C for 45 min at a pressure of 32 MPa in graphite dies lined with graphite foil that was coated with BN. A detailed description of the temperature ramp used to prepare the specimens has been reported previously.[21] A heating rate of ~10 °C/min to the hot pressing temperature was used. A mild vacuum (~20 Pa) was maintained up to 1650 °C at which time the atmosphere was switched to flowing argon. An infrared thermometer (Model OS 3708, Omega Engineering, Stanford, CT) was used to monitor the die temperature. A uniaxial load of 32 MPa was applied at 1950 °C. After holding for 45 min, the furnace was cooled at ~20 °C/min to room temperature. Billets with a diameter of ~40 mm and thickness of ~5 mm were produced. Bars with dimensions of 4 mm × 4 mm × 6 mm and 1.5 mm × 2 mm × 10 mm were sliced from the billets and ground to a 6 μm surface finish for furnace oxidation and thermal gravimetric analysis.

2.2. Oxidation

The experimental portion of this study focused on exposing ZrB_2–SiC specimens to air at temperatures of 800, 1000, 1200, 1400 and 1500 °C. A $MoSi_2$ resistance heated horizontal tube furnace (Model 0000543, Rapid Temperature Furnace, CM Inc., Bloomfield, NJ) equipped with a high purity alumina tube was used for the oxidation studies. Prior to oxidation, specimens were cleaned in an ultrasonic bath in acetone. Specimens were placed on an alumina plate which was on an alumina D-tube, inserted into the center of the furnace, and leveled. The ends of the furnace were sealed with gas-tight end caps. An atmosphere of flowing air with a volumetric flow rate of 1 cm/s through the tube relative to the specimen (~1.8 l/min based on the tube diameter of 6.35 cm) was maintained. Each specimen was heated at ~5 °C/min to the target temperature and held for 30 min. Specimen temperature was measured with a type B thermocouple that was inserted into the tube and was next to the specimen at an approximate distance of less than 2 cm. After heating to the target temperature, the specimens were cooled to room temperature at ~10 °C/min. After oxidation, the specimens that had been oxidized at 800 and 1000 °C were kept in a sealed container, which was protected from ambient moisture to prevent hydration of B_2O_3.

The oxidation behavior of ZrB_2–30 vol%SiC was also studied using thermal gravimetric analysis (TGA). The weight change was measured under flowing air at a ramp rate of 5 °C/min up to 1500 °C without an isothermal hold.

3. Characterization

The bulk density of each billet was measured using the Archimedes' technique with deionized water as the immersing medium. The relative density was determined by dividing the bulk density by the theoretical density. The microstructure of each specimen was characterized using scanning electron microscopy (SEM; S-570, Hitachi, Tokyo) along with energy dispersive spectroscopy (EDS; AAT, X-ray Optics, Gainesville, FL) for chemical analysis. For microstructural analysis, cross sections were cut perpendicular to the top surface of the oxidized bars and then polished to a 0.25 μm finish using diamond abrasives. The specimens oxidized in air at 800 and 1000 °C were polished with oil based polishing media rather than water to prevent hydration and removal of any B_2O_3 that was present. For the specimen heated to 1500 °C, grazing incidence X-ray diffraction (GXRD; X'Pert MRD, Panalytical, Almelo, Netherlands) was used to determine the crystalline phases present in the SiC-depleted region underneath the surface SiO_2-rich scale after removing the surface layers by polishing parallel to the original surface. The material removal was monitored using optical microscopy so that the desired region was reached. The incidence angle for GXRD was set to 1°, which resulted in a penetration depth of less than ~200 nm into the specimen. The GXRD employed Cu Kα radiation that was passed through a Ni filter. Grain sizes were evaluated using an imaging software program (ImageJ, U. S. National Institutes of Health, Bethesda, MD) by counting a minimum of 250 grains.

4. Results and discussion

4.1. Density

The hot-pressed billets used to produce bars for oxidation studies had measured bulk densities ranging from 5.13 to 5.18 g/cm^3. Using a rule of mixture calculation, and assuming that the true densities were 6.09 g/cm^3 for ZrB_2 and 3.21 g/cm^3 for SiC, the theoretical density of ZrB_2 containing 30 vol% SiC was calculated to be 5.23 g/cm^3. Based on this true density, all hot-pressed billets had relative densities of >98%. Consequently, porosity was not considered to have a significant effect on the oxidation behavior.

4.2. Microstructure at room temperature

A microstructure typical of the ZrB_2–SiC specimens used in this investigation is presented in Fig. 1. The darker phase is SiC and it appears to be uniformly dispersed in the lighter ZrB_2 matrix. SEM analysis did not reveal any obvious porosity in the microstructure, which supports the results of the density measurements. The average grain size of ZrB_2 was ~2.5 μm, while the SiC particles had an average diameter of ~1.7 μm. The microstructure is similar to those reported previously.[22,23]

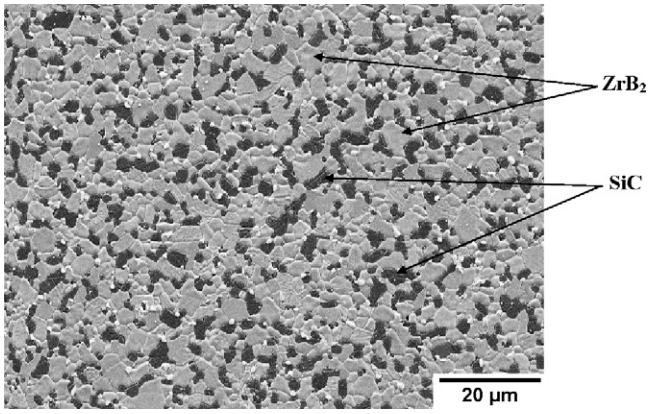

Fig. 1. SEM image of a polished, thermally etched cross section showing the microstructure of ZrB_2 containing 30 vol% SiC.

4.3. Initial response during heating (800–1200 °C)

Thermodynamically, both ZrB_2 and SiC should oxidize when exposed to air. However, the oxidation rates of both species are negligible below about 800 °C. Previous studies have reported that the oxidation of ZrB_2 by Reaction (1) is much faster than oxidation of SiC (specific reactions are discussed below) between 800 and 1200 °C.[24,25] Assuming that oxidation of ZrB_2 proceeds stoichiometrically, the reaction should produce molten B_2O_3 (melting temperature ~450 °C) and solid ZrO_2. Upon cooling to room temperature, the B_2O_3 forms an amorphous solid while the ZrO_2 is crystalline.[26]

$$ZrB_2 + \tfrac{5}{2}O_2(g) \rightarrow ZrO_2 + B_2O_3(l) \quad (1)$$

The amounts of B_2O_3 and ZrO_2 on the surface of the specimen oxidized at 800 °C for 30 min were not sufficient to be observed in polished cross sections in the SEM. Thermal gravimetric analysis, which will be discussed later in this article, did detect a small amount of oxidation of ZrB_2–SiC at 800 °C (<0.2 mg/cm^2, which corresponds to a layer <0.5 μm thick based on the mass gain and the densities of B_2O_3 and ZrO_2). For any B_2O_3 that did form, hydration and dissolution could have also led to removal of the thin reaction layer during either polishing or storage despite the steps taken to protect it from the ambient moisture.

Oxidation of ZrB_2–SiC for 30 min at 1000 °C led to the formation of enough B_2O_3 and ZrO_2 so that they could be observed in SEM micrographs (Fig. 2). At this temperature, the surface structure consisted of: (1) a layer of B_2O_3 ~2 μm thick, (2) a ZrO_2 layer ~6 μm thick that contained unoxidized SiC and (3) unaffected ZrB_2–SiC. A continuous B_2O_3 layer was found to form above the ZrO_2 layer. This structure may form due to volume expansion upon conversion of ZrB_2 to ZrO_2 and B_2O_3 (~300% volume expansion based on density calculations) and/or the mutual wetting behavior of the two materials. Because the oxidation of SiC is much slower than that of ZrB_2 in this temperature regime, the SiC particles did not oxidize appreciably. As ZrB_2 oxidized, SiC particles were embedded in the growing ZrO_2 layer (Fig. 2). The composition of the layer labeled ZrO_2 + SiC was examined using EDS mapping (Fig. 3), which showed that zirconium and oxygen were present along with silicon, suggesting that the reaction layer was composed of ZrO_2 and SiC. Determination of the composition of the outermost layer by EDS was not possible due to its low sensitivity to light elements (i.e. boron). However, EDS analysis reported by other investigators has shown that the outermost layer contained O, but was free of Si and Zr, which is consistent with the presence of B_2O_3.[25–28] Earlier studies have also concluded that B_2O_3 was an effective barrier to the transport of oxygen, leading to passive oxidation behavior with parabolic mass gain kinetics,[24–28] which is consistent with the structure observed in the current study (Fig. 2). Passive oxidation protection is provided by the continuous molten B_2O_3 layer that effectively seals the surface and prevents direct exposure of the ZrB_2–SiC to air in this temperature regime.[28]

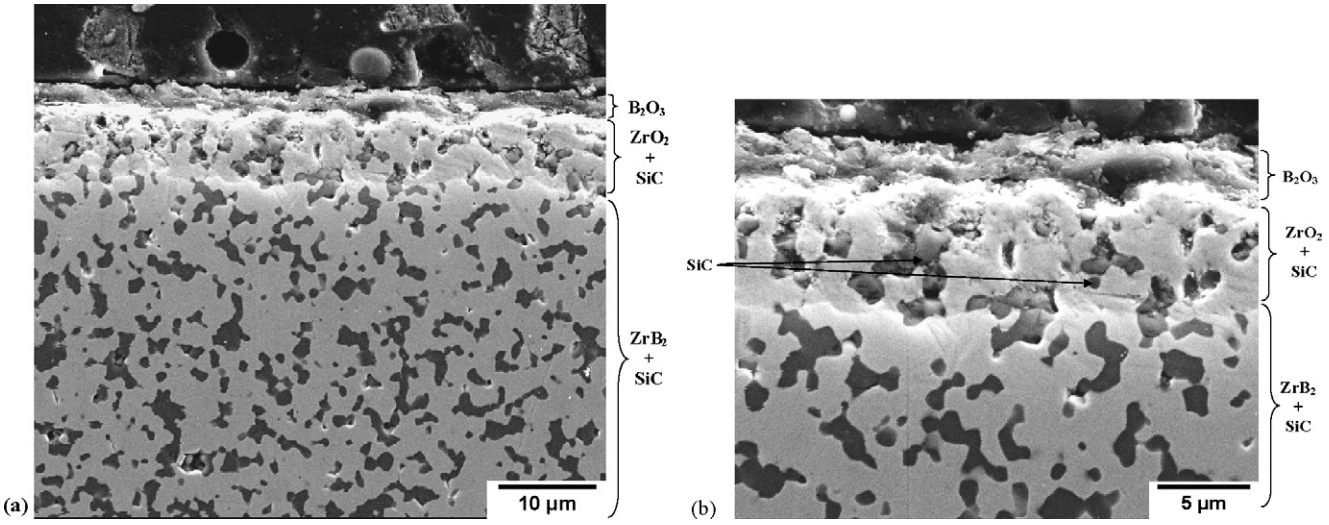

Fig. 2. SEM images at (a) low and (b) high magnification showing a layer of B_2O_3 ~2 μm thick and a layer of ZrO_2–SiC ~6 μm thick formed on the surface of ZrB_2–SiC after exposure to air at 1000 °C for 30 min.

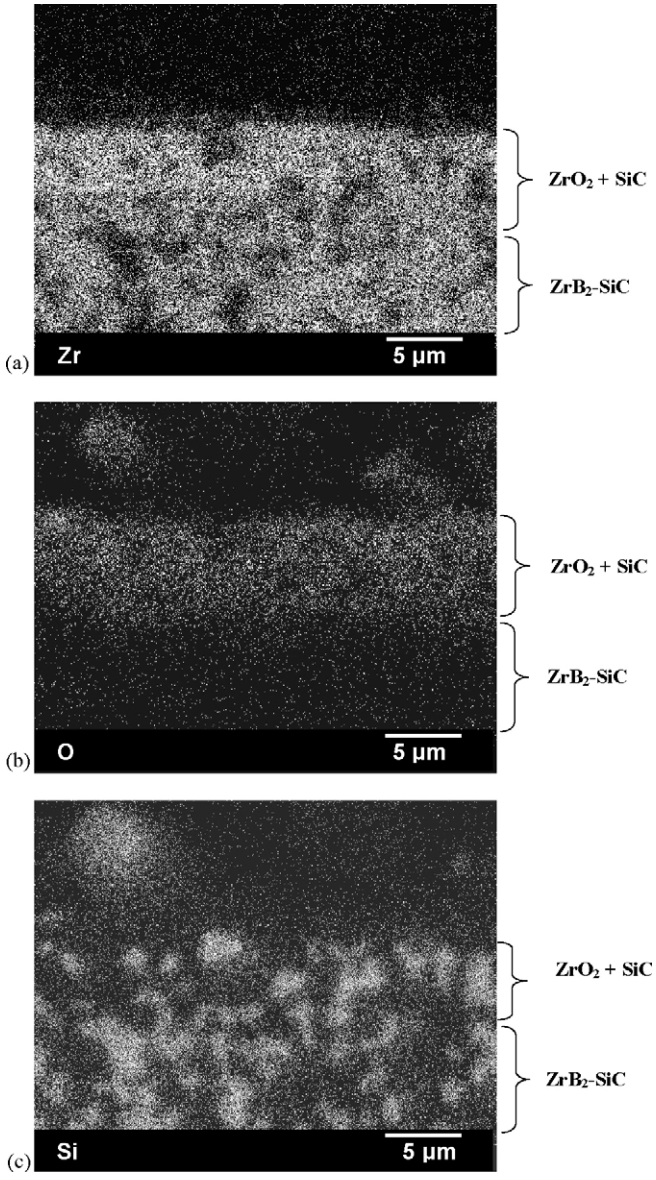

Fig. 3. EDS maps for (a) Zr, (b) O and (c) Si for the reaction layer formed by oxidizing ZrB_2–SiC at 1000 °C in air for 30 min showing that a layer that contains Zr, O and Si is formed.

4.4. Transition structure

As ZrB_2–SiC was heated above ~1200 °C, the composition and structure of the surface layers changed. The dominant chemical processes between 1200 and 1400 °C are expected to be the evaporation of B_2O_3 (Reaction (2)) and oxidation of SiC (Reaction (3)).

$$B_2O_3(l) \rightarrow B_2O_3(g) \quad (2)$$

$$SiC + \tfrac{3}{2}O_2(g) \rightarrow SiO_2(l) + CO(g) \quad (3)$$

As the temperature approaches 1400 °C, the vapor pressure of B_2O_3 increases substantially,[8] leading to its rapid evaporation. In addition, SiC starts to oxidize producing molten SiO_2 and gaseous species such as CO in this temperature regime. Like oxidation at lower temperatures, heating to 1200 °C for 30 min resulted in the formation of a continuous surface layer above another oxide layer (Fig. 4). In this case, the underlying layer was composed of porous ZrO_2. A thin SiO_2-rich layer (<1 μm) covered the underlying material and could, potentially, provide a barrier to oxygen diffusion that may result in passive oxidation protection with parabolic mass gain kinetics. This SiO_2-rich layer is expected to contain some B_2O_3 during transient heating to 1500 °C based on either incomplete evaporation of the B_2O_3 by Reaction (2) or the continued production of B_2O_3 beneath the outer scale by Reaction (1). Compositional analysis of the outermost layer using secondary ion mass spectrometry (SIMS) has shown that the B content of the oxide layer after heating to 1500 °C for 30 min is less than 1 wt%.[23]

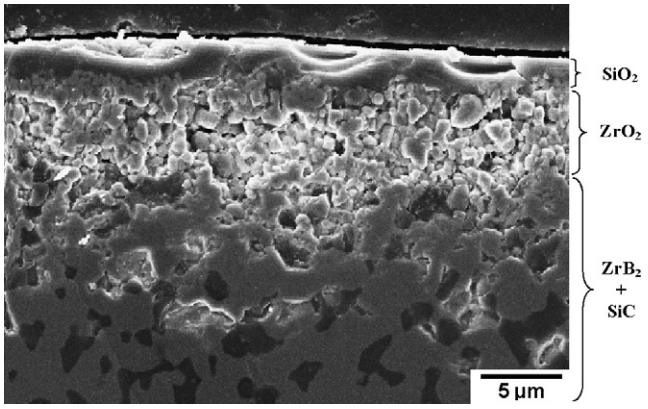

Fig. 4. SEM image showing the formation of an outer layer of SiO_2 and a second layer composed of ZrO_2 on the surface of ZrB_2–SiC after exposure to air at 1200 °C for 30 min.

The structure formed at 1400 °C in the current study (Fig. 5) is consistent with literature reports that indicate that B_2O_3 evaporates rapidly at temperatures above 1100 °C.[28] When the evaporating B_2O_3 is not replaced, as is the case for monolithic ZrB_2, the effectiveness of the diffusion barrier is reduced since the porous ZrO_2 layer alone does not protect the underlying ZrB_2 from rapid oxidation. For ZrB_2–SiC, the addition of SiC extends the oxidation resistance to higher temperatures by promoting the formation of a borosilicate glass layer on exposed surfaces. Previous studies have reported that a SiO_2-rich layer provides passive oxidation protection with parabolic mass gain kinetics, reducing the oxidation rate compared to pure ZrB_2 at temperatures above 1200 °C.[1,24,29] In the present furnace oxidation studies, formation of SiO_2 was first observed for the 1200 °C specimen (detected by EDS), which is consistent with the previous reports.[24]

As the temperature approached 1400 °C, the thickness of the SiO_2 layer on the surface increased to ~10 μm (Fig. 5). The thickness of the SiO_2 layer, and the underlying ZrO_2-containing layer were not uniform over the specimen surface at this temperature. This may be due to wetting characteristics or other local variations such as composition, surface topology or surface cracks that might enhance the local oxidation rate. The ZrO_2 layer was thicker in the areas where the SiO_2 layer was thinner, indicating less effective oxidation protection in those regions.

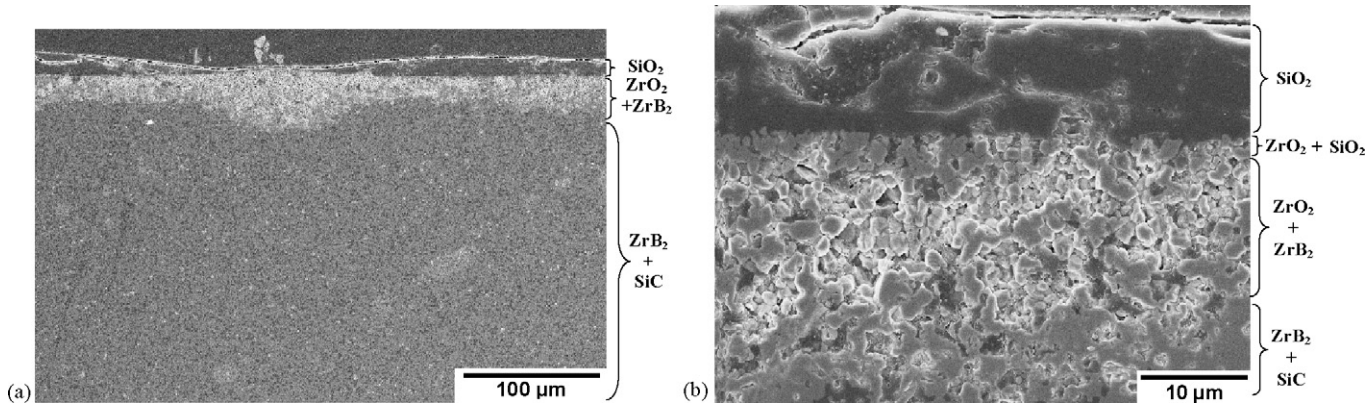

Fig. 5. SEM images at (a) low and (b) high magnification of the layered structure formed after exposure of ZrB_2–SiC to air at 1400 °C for 30 min.

4.5. Evolution as temperature approaches 1500 °C

The structure of the specimen heated in air to 1500 °C (Fig. 6) for 30 min was similar to the structure of the specimen exposed to 1400 °C, except that the reaction layers were thicker and more uniform after heating to 1500 °C. The thickness of the SiO_2-rich layer was ~10 μm after heating to 1500 °C with a hold of 30 min. At this temperature, the layered structure consisted of: (1) a SiO_2-rich glassy layer; (2) a thin layer of ZrO_2–SiO_2; (3) a layer of ZrO_2 and/or ZrB_2 from which SiC had been partially depleted; (4) unaffected ZrB_2–SiC. This layered structure is similar to the structure reported for ZrB_2–SiC exposed to air at 1500 or 1627 °C in other studies.[16,17]

Based on isothermal studies, the SiO_2-rich glassy layer remains protective up to at least 1500 °C.[1,16,18] Because SiO_2 is significantly less volatile than B_2O_3 at these temperatures (the vapor pressure of B_2O_3 is $\sim 10^5$ times higher than that of SiO_2 at 1500 °C), the SiO_2-rich layer provides oxidation protection for ZrB_2–SiC over a much greater temperature range than the B_2O_3 does for pure ZrB_2.[23]

A ZrO_2–SiO_2 layer with what appears to be a two phase, interpenetrating microstructure formed beneath the SiO_2 layer as the temperature approached 1500 °C (Fig. 6). Apparently, the porous ZrO_2 that formed initially through oxidation of ZrB_2 between 800 and 1200 °C was retained, but was covered and partially filled with SiO_2 that formed through oxidation of SiC at higher temperatures. Although quantitative analysis was not possible by EDS since B is at the limit of the detection capability or by XRD since the B_2O_3 is amorphous, some B_2O_3 probably remained dissolved in the SiO_2 in this layer, although a previous SIMS investigation showed the amount to be minimal.[23] The ZrO_2–SiO_2 layer was relatively thin (<3 μm). Experiments that have employed thermal cycling appear to promote growth of the ZrO_2–SiO_2 layer, but no mechanism has been proposed for the formation or growth of this layer.[16] Diffusion of oxygen molecules or ions through the SiO_2 and ZrO_2–SiO_2 layers is thought to be the rate determining step in the oxidation of ZrB_2–SiC. Materials with coherent SiO_2 and/or ZrO_2–SiO_2 layers exhibit passive oxidation behavior with parabolic mass gain kinetics at 1500 °C due to the stability of SiO_2 in air in this temperature regime.[23,24]

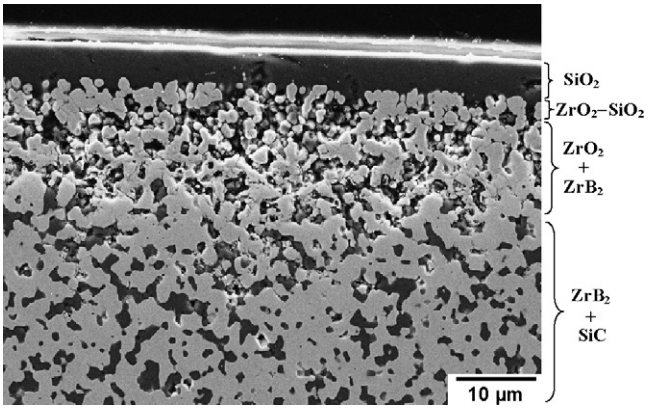

Fig. 6. SEM image of the layered structure formed after exposure of ZrB_2–SiC to air at 1500 °C for 30 min.

A SiC-depleted region, which was located underneath the ZrO_2–SiO_2 layer, had a porous structure from which the SiC has been partially or entirely removed (Fig. 6). The morphology of the grains in this region was similar to the original structure before oxidation, except that the SiC had been partially or fully removed by active oxidation. The thickness of the depleted region was ~10 μm after heating to 1500 °C for 30 min.

Grazing incidence X-ray diffraction analysis was used to examine the crystalline phases present in oxidized specimens that had been observed in cross section. After removing the outer SiO_2 layer and the ZrO_2–SiO_2 layer through successive polishing, analysis showed that the SiC-depleted layer was composed of a mixture of ZrO_2 and ZrB_2 from which some or all of the SiC had been removed (Fig. 7). This result suggests that an oxygen partial pressure (activity) gradient exists across the SiC-depleted layer. In addition, thermodynamic analysis has suggested that the SiO(g) that is generated as SiC is oxidized (Reaction (4) or (5)) is transported across the SiC-depleted layer due to this oxygen partial pressure gradient.[20] Since a p_{O_2} gradient is thought to exist across the SiC-depleted layer, an interface separating a layer where ZrO_2 is dominant from a layer in which ZrB_2 is dominant may be located either: (1) at the interface of the unoxidized ZrB_2–SiC and the SiC-depleted layer, (2) in the SiC-depleted layer or (3) at the interface between the SiC-depleted layer and the ZrO_2–SiO_2 layer. A more detailed analysis is needed

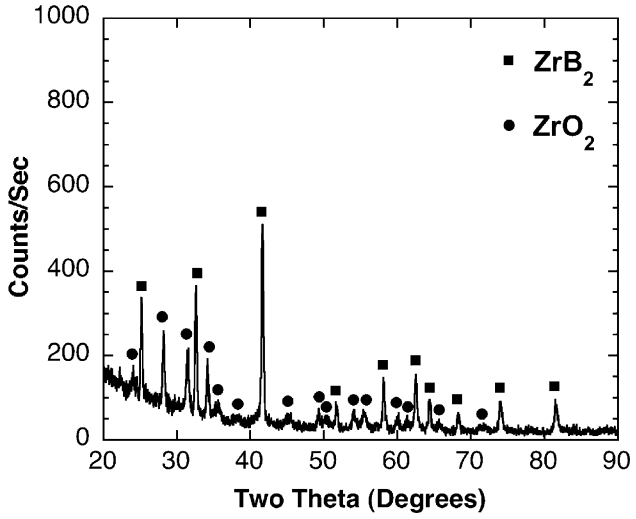

Fig. 7. Grazing incidence XRD of the SiC-depleted layer formed by oxidation of ZrB_2–SiC in air at 1500 °C.

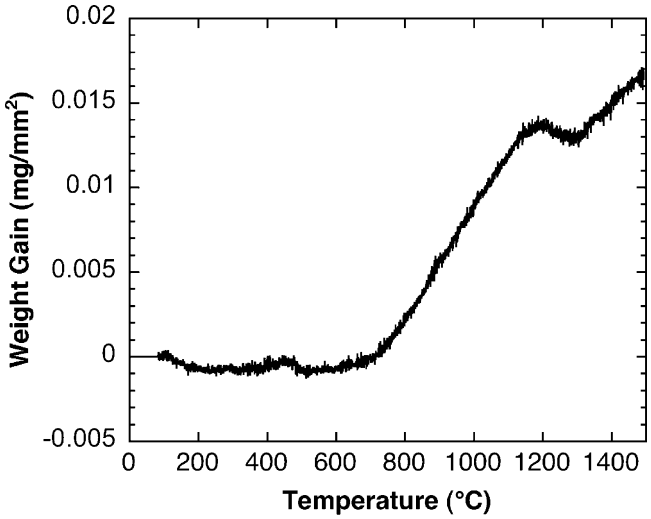

Fig. 8. TGA analysis of ZrB_2–SiC in air up to 1500 °C.

to identify a distinguishable interface.

$$SiC + O_2(g) \rightarrow SiO(g) + CO(g) \quad (4)$$

$$SiO(g) + \tfrac{1}{2}O_2(g) \rightarrow SiO_2(l) \quad (5)$$

Formation of the SiC-depleted layer in ZrB_2–SiC specimens exposed to air at 1500 °C has been analyzed using volatility diagrams and thermodynamic calculations.[20] At intermediate oxygen partial pressures ($p_{O_2} \sim 10^{-10}$ to 10^{-15} Pa) that are thought to exist in the SiC-depleted layer, SiC should undergo active oxidation by Reaction (4) or a similar process. The SiO(g) that is formed by active oxidation is transported from the SiC surface (high $p_{SiO(g)}$ and low p_{O_2}) to the SiO_2 layer (low $p_{SiO(g)}$ and high p_{O_2}) due to the chemical potential gradients of O_2 and SiO(g) across the depleted region. At the interface between the SiC-depleted region and the SiO_2-containing layer, the SiO(g) could either oxidize to form additional SiO_2 or diffuse into the layer and react with dissolved oxygen to form SiO_2 closer to the surface of the outer SiO_2 layer.

Based on the thermodynamic analysis and the observations reported in this paper, the dominant chemical process in the SiC-depleted layer at 1500 °C appears to be the active oxidation of SiC (Reaction (4)) which results in the depletion of SiC.

4.6. Thermal gravimetric analysis (TGA)

To complement the compositional and structural information, the oxidation behavior of the ZrB_2–SiC was examined by TGA up to 1500 °C with the same heating rate (5 °C/min) that was used in the furnace oxidation experiments. The change in the mass as a function of temperature is shown in Fig. 8. The weight started to increase just below ~800 °C, which corresponds to the temperature at which ZrB_2 is reported to begin oxidizing.[24,25,28] The weight gain was consistent with SEM analysis that showed a minimal amount of B_2O_3 formation for specimens heated in air to ~800 °C (<0.2 mg/cm^2), but thicker oxide layers at higher temperatures. Between 700 and 1200 °C, the weight increased at a constant rate (~3.3×10^{-3} mg/cm^2 °C). This is consistent with SEM observations that showed formation and growth of ZrO_2 and a protective layer of B_2O_3 (Figs. 2 and 3). As the temperature approached 1200 °C the specimen weight decreased slightly, with a mass loss rate of ~1.0×10^{-3} mg/cm^2 °C between 1215 and 1300 °C. The mass loss was attributed to a significant increase in the rate of volatilization of B_2O_3.[8] Even though the specimen mass decreased in this temperature regime, analysis by EDS verified that SiO_2 was present after oxidation at 1200 °C whereas no silicon was detected on the surface after oxidation at 1000 °C (Fig. 3). Thus, SiO_2 is formed at ~1200 °C, but the rate of formation must have been less than the rate of evaporation of B_2O_3 since an overall mass loss was observed by TGA. Above ~1300 °C the specimen mass increased with a mass gain rate of ~1.8×10^{-3} mg/cm^2 °C. Based on SEM observations and other analysis, the mass gain was due, primarily, to the formation of SiO_2.

5. Summary

The changes in structure for ZrB_2–SiC during heating to 1500 °C in air were examined using furnace oxidation followed by SEM/EDS and XRD analysis. Thermal gravimetric analysis was also employed to evaluate the mass change as a function of temperature. Between 800 and 1200 °C, oxidation of ZrB_2 to ZrO_2 and B_2O_3 was the dominant chemical process. TGA showed that the weight gain started just below 800 °C. This resulted in passive oxidation behavior due to the protection provided by the formation of a continuous molten B_2O_3 layer. Weight gain continued at a constant rate (~3.3×10^{-3} mg/cm^2 °C) up to ~1200 °C. At ~1200 °C, oxidation of SiC was initiated resulting in the formation of SiO_2. In addition, the evaporation of B_2O_3 became rapid resulting in a weight loss recorded by TGA (~1.0×10^{-3} mg/cm^2 °C). The B_2O_3 was depleted by ~1300 °C, which resulted in mass gain above this temperature due to SiO_2 formation. Oxidation of SiC continued up to 1500 °C and the thickness of the SiO_2-rich scale increased to a maximum of ~10 μm. At 1500 °C, a layered structure is formed that consisted of: (1) a continuous SiO_2-rich

layer (∼10 μm); (2) a Zr-rich oxidized layer embedded in amorphous SiO_2 (<3 μm); (3) a layer of SiC-depleted ZrB_2 and ZrO_2 (∼10 μm); (4) unaffected ZrB_2–SiC. The observed increase in the thickness of the outer SiO_2 layer required several steps including: (1) the active oxidation of SiC in the SiC-depleted region; (2) transport of SiO(g) across the SiC-depleted region; (3) re-oxidation of SiO(g) to SiO_2. Through the entire temperature range, ZrB_2–SiC exhibited passive oxidation behavior in which the diffusion of oxygen through protective molten layers containing B_2O_3 and/or SiO_2 controlled the rate of oxidation.

Acknowledgements

The material presented in this paper is based upon the work supported by the National Science Foundation under grant number DMR-0346800. Additionally, the use of the Advanced Materials Characterization Laboratory at UMR and in particular assistance from Dr. Scott Miller is gratefully acknowledged.

References

1. Levine, S. R., Opila, E. J., Halbig, M. C., Kiser, J. D., Singh, M. and Salem, J. A., Evaluation of ultra high temperature ceramics for aeropropulsion use. *J. Eur. Ceram. Soc.*, 2002, **22**, 2757–2767.
2. Monteverde, F. and Bellosi, A., Development and characterization of metal-diboride-based composites toughened with ultra-fine SiC particulates. *Solid State Sci.*, 2005, **7**, 622–630.
3. Monteverde, F. and Bellosi, A., The resistance to oxidation of an HfB_2–SiC composite. *J. Eur. Ceram. Soc.*, 2005, **25**, 1025–1031.
4. Opeka, M. M., Talmy, I. G. and Zaykoski, J. A., Oxidation-based materials selection for 2000 °C + hypersonic aerosurfaces: theoretical considerations and historical experience. *J. Mater. Sci.*, 2004, **39**, 5887–5904.
5. Van Wie, D. M., Drewry, D. G., King, D. E. and Hudson, C. M., The hypersonic environment: required operating conditions and design challenges. *J. Mater. Sci.*, 2004, **39**, 5915–5924.
6. Chamberlain, A. L., Fahrenholtz, W. G. and Hilmas, G. E., Oxidation of ZrB2–SiC ceramics under atmospheric and reentry conditions. *Refract. Appl. Trans.*, 2005, **1**, 1–8.
7. Sciti, D., Brach, M. and Bellosi, A., Oxidation behavior of a pressureless sintered ZrB_2–$MoSi_2$ ceramic composite. *J. Mater. Res.*, 2005, **20**, 922–930.
8. Monteverde, F. and Bellosi, A., Oxidation of ZrB_2-based ceramics in dry air. *J. Electrochem. Soc.*, 2003, **150**, B552–B559.
9. Nguyen, Q. N., Opila, E. J. and Robinson, R. C., Oxidation of ultra high temperature ceramics in water vapor. *J. Electrochem. Soc.*, 2004, **151**, B558–B562.
10. Bartuli, C., Valente, T. and Tului, M., High temperature behavior of plasma sprayed ZrB_2–SiC composite coatings. In *Thermal Spray 2001: New Surfaces for a New Millennium, Proceedings of the International Thermal Spray Conference, Singapore*. ASM International, Materials Park, OH, USA, 2001, pp. 259–262.
11. Valente, T., Marino, G. and Tului, M., Mechanical properties of ceramic matrix composite for high temperature applications obtained by plasma spraying. In *Thermal Spray 2004: Advances in Technology and Application, Proceedings of the International Thermal Spray Conference*. ASM International, Materials Park, OH, USA, 2001, pp. 32–35.
12. Kaji, N., Shikano, H. and Tanaka, I., Development of ZrB_2–graphite protective sleeve for submerged nozzle. *Taikabutsu Overseas*, 1992, **14**, 39–43.
13. Kinoshita, S., Yoshimasa, Y. and Ono, Y., Application of zirconium boride materials to waste melting furnace. In *Proceedings of International Conference on Refractories, UNITECR'03*, 2003, pp. 205–208.
14. Prietzel, S., Hunold, K., Potscke, J. and Kross, U., Submerged entry nozzles containing zirconium diboride. In *Proceedings of International Conference on Refractories, UNITECR'01*, 2001, pp. 983–992.
15. Cutler, R. A., *Ceramics and Glasses Engineered Materials Handbook*, *vol. 4*, ed. S. J. Schneider Jr. ASM International, Materials Park, OH, 1991, pp. 787–803.
16. Opila, E. J., Levine, S. and Lorincz, J., Oxidation of ZrB_2- and HfB_2-based ultra-high temperature ceramics: effect of Ta additions. *J. Mater. Sci.*, 2004, **39**, 5969–5977.
17. Kaufman, L., Clougherty, E. V. and Berkowitz-Mattuck, J. B., Oxidation characteristics of hafnium and zirconium diboride. *Trans. Met. Soc. AIME*, 1967, **239**, 458–466.
18. Gasch, M., Ellerby, D., Irby, E., Beckman, S., Gusman, M. and Johnson, S., Processing, properties, and arc jet oxidation of hafnium diboride/silicon carbide ultra high temperature ceramics. *J. Mater. Sci.*, 2004, **39**, 5925–5937.
19. Opila, E. J. and Halbig, M. C., Oxidation of ZrB_2–SiC. *Ceram. Eng. Sci. Proc.*, 2001, **22**, 221–228.
20. Fahrenholtz, W. G., Thermodynamic analysis of ZrB2–SiC oxidation: formation of a SiC-depleted region. *J. Am. Ceram. Soc.*, in press.
21. Chamberlain, A. L., Fahrenholtz, W. G., Hilmas, G. E. and Ellerby, D. T., High strength zirconium diboride-based ceramics. *J. Am. Ceram. Soc.*, 2004, **87**, 1170–1172.
22. Rezaie, A. R., Fahrenholtz, W. G. and Hilmas, G. E., Effect of hot pressing time and temperature on the microstructure and mechanical properties of ZrB2–SiC. *J. Mater. Sci.*, doi:10.1111/j.1551-2916.2006.01329.x, in press.
23. Rezaie, A. R., Fahrenholtz, W. G. and Hilmas, G. E., Oxidation of zirconium diboride–silicon carbide at 1500 °C a low partial pressure of oxygen. *J. Am. Ceram. Soc.*, 2006, **89**(10), 3240–3245.
24. Tripp, W. C., Davis, H. H. and Graham, H. C., Effect of an SiC addition on the oxidation of ZrB_2. *Am. Ceram. Soc. Bull.*, 1973, **52**, 612–613.
25. Tripp, W. C. and Graham, H. C., Thermogravimetric study of the oxidation of ZrB_2 in the temperature range of 800–1500 °C. *J. Electrochem. Soc.*, 1968, **118**, 1195–1199.
26. Kuriakose, A. K. and Margrave, J. L., The oxidation kinetics of zirconium diboride and zirconium carbide at high temperatures. *J. Electrochem. Soc.*, 1964, **111**, 827–8331.
27. Berkowitz-Mattuck, J. B., High-temperature oxidation. III: Zirconium and hafnium diborides. *J. Electrochem. Soc.*, 1966, **113**, 908–914.
28. Irving, R. J. and Worsley, I. G., Oxidation of titanium diboride and zirconium diboride at high temperatures. *J. Less-Common Met.*, 1968, **16**, 102–112.
29. Opeka, M. M., Talmy, I. G., Wuchina, E. J., Zaykoski, J. A. and Causey, S. J., Mechanical, thermal, and oxidation properties of hafnium and zirconium compounds. *J. Eur. Ceram. Soc.*, 1999, **19**, 2405–2414.